Charge ordering in θ-(BEDT-TTF)$_2$RbZn(SCN)$_4$:
Cooperative effects of electron correlations and lattice distortions

Satoshi Miyashita[1,2*] and Kenji Yonemitsu[2,3]

[1]*Institute for Materials Research, Tohoku University, Sendai 980-8577, Japan*
[2]*Institute for Molecular Science, Okazaki 444-8585, Japan*
[3]*Department of Functional Molecular Science, Graduate University for Advanced Studies, Okazaki 444-8585, Japan*
(Dated: February 1, 2008)

Combined effects of electron correlations and lattice distortions are investigated on the charge ordering in θ-(BEDT-TTF)$_2$RbZn(SCN)$_4$ theoretically in a two-dimensional 3/4-filled extended Hubbard model with electron-lattice couplings. It is known that this material undergoes a phase transition from a high-symmetry metallic state to a low-symmetry insulating state with a horizontal-stripe charge order (CO) by lowering temperature. By means of the exact-diagonalization method, we show that electron-phonon interactions are crucial to stabilize the horizontal-stripe CO and to realize the low-symmetry crystal structure.

I. INTRODUCTION

Two-dimensional (2D) strongly correlated electron systems have attracted much attention in condensed matter physics. For bis(ethylenedithio)-tetrathiafulvalene (BEDT-TTF) salts, which are 2D strongly correlated organic conductors with various molecular arrangements,[1,2] many theoretical scientists use the extended Hubbard model in order to understand the role played by long-range Coulomb interactions. It should be noted that not only electron-electron interactions but also electron-phonon couplings can be significant because the crystal structure is often altered at a phase transition. These materials exhibit many interesting phenomena such as metal-insulator (M-I) transitions with charge ordering, the realization of a spin liquid state,[3] superconductivity,[4] and so on. In particular, transitions to states with a charge order (CO) have been investigated theoretically[5,6,7,8,9] and experimentally.[10,11]

θ-(BEDT-TTF)$_2$RbZn(SCN)$_4$ (called θ-RbZn for simplicity hereafter) is a representative compound which undergoes a CO transition accompanied with a structural deformation by lowering temperature.[10,11] The ground state of the θ-RbZn salt is an insulator with the horizontal-stripe CO along t_{p4} bonds (HCO-t_{p4}) shown in Fig. 1(b), where sites 1 and 4 are hole-rich, as confirmed by the X-ray structural analysis,[12] ^{13}C-NMR measurements[13,14] and polarized Raman and IR spectroscopy.[15,16] The importance of long-range electron-electron interactions is well recognized and the mechanism for stabilizing the HCO-t_{p4} has been argued mainly on the basis of the low-symmetry structure. Because the lattice distortions are coupled with the electron system, giving rise to the first-order transition sensitive to the crystal structure, electron-phonon interactions are also important.

Quite recently, Iwai *et al.* have observed photoinduced melting of CO in the θ-RbZn salt and in α-(BEDT-TTF)$_2$I$_3$ (called α-I$_3$ for simplicity hereafter) by femtosecond reflection spectroscopy.[17] The θ-RbZn and α-I$_3$ salts show large and small molecular rearrangements, respectively, at the M-I transition. Their photoinduced dynamics are qualitatively different: the θ-RbZn salt shows local melting of CO and ultrafast recovery of CO irrespective of temperature and excitation intensity, while the α-I$_3$ salt shows critical slowing down. Thus, it is important to show how electron-phonon interactions are significant in the θ-RbZn salt.

This paper is organized as follows. After a brief explanation of the model in the next section, we present the exact-diagonalization results in Sec.III for the hole-hole correlation functions, the hole densities, and the modulations of transfer integrals, from which we propose that the low-symmetry structure of the θ-RbZn salt at low temperature is reproduced by introducing electron-lattice couplings in the model based on the high-symmetry structure at high temperature. Then, in Sec.IV, we discuss the numerical results on the basis of a perturbation theory from the strong-coupling limit. A brief summary is given in Sec.V.

II. MODEL

We start with the following extended Hubbard model at 3/4-filling with electron-phonon couplings of transfer-modulation type,

$$\mathcal{H} = \sum_{\langle i,j \rangle} \sum_{\mu=c,p1,p4} \left[t_{i,j} \pm \alpha_\mu u_\mu \right] c^\dagger_{i,\sigma} c_{j,\sigma} + U \sum_i n_{i,\uparrow} n_{i,\downarrow}$$
$$+ V_c \sum_{\langle i,j \rangle_c} n_i n_j + V_p \sum_{\langle i,j \rangle_p} n_i n_j + \sum_{\mu=c,p1,p4} \frac{K_\mu}{2} u_\mu^2 \quad (1)$$

where $c^\dagger_{i,\sigma}$ creates an electron with spin σ at site i, $n_{i,\sigma} = c^\dagger_{i,\sigma} c_{i,\sigma}$, and $n_i = \sum_\sigma n_{i,\sigma}$. $t_{i,j} = t_c^{\text{HT}}$, t_{p1}^{HT} or t_{p4}^{HT} is the transfer integral for the bond between the i-th site and its nearest-neighbor j-th site along the c, $p1$ or $p4$ bond. $\langle i,j \rangle_c$ and $\langle i,j \rangle_p$ denote the nearest-neighbor
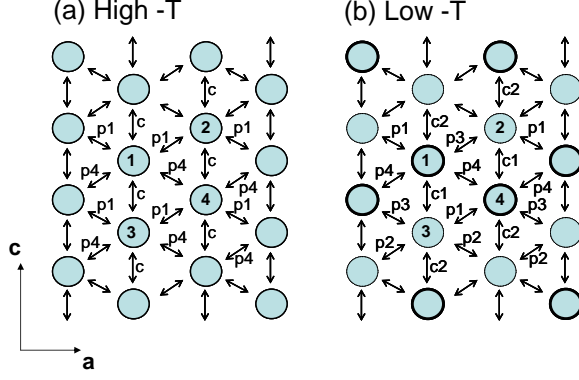
FIG. 1: (Color online) Anisotropic triangular lattice for θ-RbZn salt: (a) high-symmetry structure at high temperature, and (b) low-symmetry structure at low temperature with horizontal-stripe CO along t_{p4} bonds. The thin and thick circles represent the hole-poor and the hole-rich sites, respectively.

pairs i and j along the c bond and the p bond, respectively. U represents the on-site Coulomb interaction, and $V_{c(p)}$ is the intersite Coulomb interaction between the i-th site and the j-th site on the $c(p)$-bond. u_i is the i-th molecular translation or rotation explained later from the equilibrium position in the high temperature phase. α_μ and K_μ are the electron-phonon coupling strength and the elastic coefficient, respectively. For simplicity, we perform variable transformations as

$$\alpha_\mu u_\mu = y_\mu , \quad \frac{\alpha_\mu^2}{K_\mu} = s_\mu . \tag{2}$$

III. NUMERICAL RESULTS

We show energy values in the unit of electron volt (eV) in the following. For electron-phonon couplings, we consider three kinds of molecular displacements: translations in the c-direction (u_c), those in the a-direction (u_{p1}), and rotations (u_{p4}) as discussed in terms of elevation angles by Watanabe et al.[12] We suppose that translations in the $c(a)$-direction contribute to modulations of the transfer integrals on the $c1$-($p1$-) and $c2$-($p3$-)bonds. We also assume that molecular rotations produce differences between the transfer integral on the $p2$-bond and that on the $p4$-bond. Then, the modulated transfer integral on each bond reads

$$\begin{aligned}
t_{c1} &= t_c^{\mathrm{HT}} - \alpha_c u_c , \quad t_{c2} = t_c^{\mathrm{HT}} + \alpha_c u_c , \\
t_{p1} &= t_{p1}^{\mathrm{HT}} + \alpha_{p1} u_{p1} , \quad t_{p3} = t_{p1}^{\mathrm{HT}} - \alpha_{p1} u_{p1} , \\
t_{p2} &= t_{p4}^{\mathrm{HT}} + \alpha_{p4} u_{p4} , \quad t_{p4} = t_{p4}^{\mathrm{HT}} - \alpha_{p4} u_{p4} .
\end{aligned} \tag{3}$$

The signs here are so determined that $y_\mu > 0$ corresponds to a deviation from the high-temperature crystal structure toward the low-temperature one of the θ-RbZn salt.

In this section, we adopt $U = 0.7$ and $V_c, V_p \leq U/2$.[18,19,20] Typical values for transfer integrals t_μ in

BEDT-TTF salts are estimated from the extended Hückel calculation.[21] We suppose here from the experimental data[12] that $t_c^{\mathrm{HT}} = 0.035$, $t_{p1}^{\mathrm{HT}} = 0.095$, and $t_{p4}^{\mathrm{HT}} = -0.095$ correspond to the high-symmetry structure at high temperature, where the $p1$ and $p4$ bonds are equivalent.

We use the exact-diagonalization method for electrons, regard phonons as classical variables, and apply the Hellmann-Feynman theorem to impose the self-consistency condition on the phonons (y_c, y_{p1}, y_{p4}) determined by

$$\langle \frac{\partial \mathcal{H}}{\partial y_\mu} \rangle = 0 . \tag{4}$$

We vary mainly coupling strengths, s_c, s_{p1}, and s_{p4}.

A. Case without electron-phonon couplings

At the beginning, we clarify the ground-state properties of the model (1) in the absence of lattice distortions. In this case, the exact-diagonalization studies of the 4×4-site cluster show that the hole densities are uniform ($\langle n_i^h \rangle = 1 - \langle n_i \rangle = 0.5$) in any combination of V_c and V_p (not shown). Degenerate CO states are mixed owing to the finite-size effect. Then, we have calculated correlation functions in this cluster.

Figure 2 shows the hole-hole correlation functions without electron-phonon couplings on the $V_c - V_p$ plane. $\langle n_i^h n_{i+1(i+2)}^h \rangle_\mu$ denotes the hole-hole correlation function along the μ-bond between the i-th and its neighbor (its second-neighbor) site. $\langle n_i^h n_j^h \rangle_\mu$ being nearly equal to 0.5 means that $(\langle n_i^h \rangle, \langle n_j^h \rangle) = (1 - \delta, 1 - \delta)$ is equally mixed with (δ, δ) with small δ. On the other hand, very small $\langle n_i^h n_j^h \rangle_\mu$ represents that $(\langle n_i^h \rangle, \langle n_j^h \rangle) = (1 - \delta, \delta)$ is mixed with $(\delta, 1 - \delta)$. Namely, $\langle n_i^h n_j^h \rangle$ is close to 0 (0.5) when the charge disproportionation between the i-th and the j-th sites is large (small).

For large V_c, e.g., for $(V_c, V_p) = (0.35, 0.01)$, $\langle n_i^h n_{i+1}^h \rangle_c \sim 0.05$, $\langle n_i^h n_{i+2}^h \rangle_c \sim 0.44$, $\langle n_i^h n_{i+1}^h \rangle_p \sim 0.23$, and $\langle n_i^h n_{i+2}^h \rangle_p \sim 0.39$. This result means that the diagonal-stripe CO is the largest at this point among all hole-hole correlations. On the other hand, for small V_c, e.g., for $(V_c, V_p) = (0.01, 0.35)$, $\langle n_i^h n_{i+1}^h \rangle_c \sim 0.46$, $\langle n_i^h n_{i+2}^h \rangle_c \sim 0.46$, $\langle n_i^h n_{i+1}^h \rangle_p \sim 0.03$, and $\langle n_i^h n_{i+2}^h \rangle_p \sim 0.46$. Here, the vertical-stripe CO is the largest correlation. In the ground state with comparable V_c and V_p, the diagonal- and the vertical-stripe COs coexist. Regarding the steep variation in the contour plots of the correlation functions in Fig. 2 as a phase boundary, we obtain the ground-state phase diagram on the V_c-V_p plane in Fig. 3. The phase diagram consists of three uniform phases with different hole-hole correlations; the coexistent phase (I), the phase with dominant vertical-stripe CO correlation (II), and the phase with dominant diagonal-stripe CO correlation (III). This phase diagram is consistent with the previous work.[22] The most important thing here is

(a) $\langle n_i^h n_{i+1}^h \rangle_c$

(b) $\langle n_i^h n_{i+2}^h \rangle_c$

(c) $\langle n_i^h n_{i+1}^h \rangle_p$
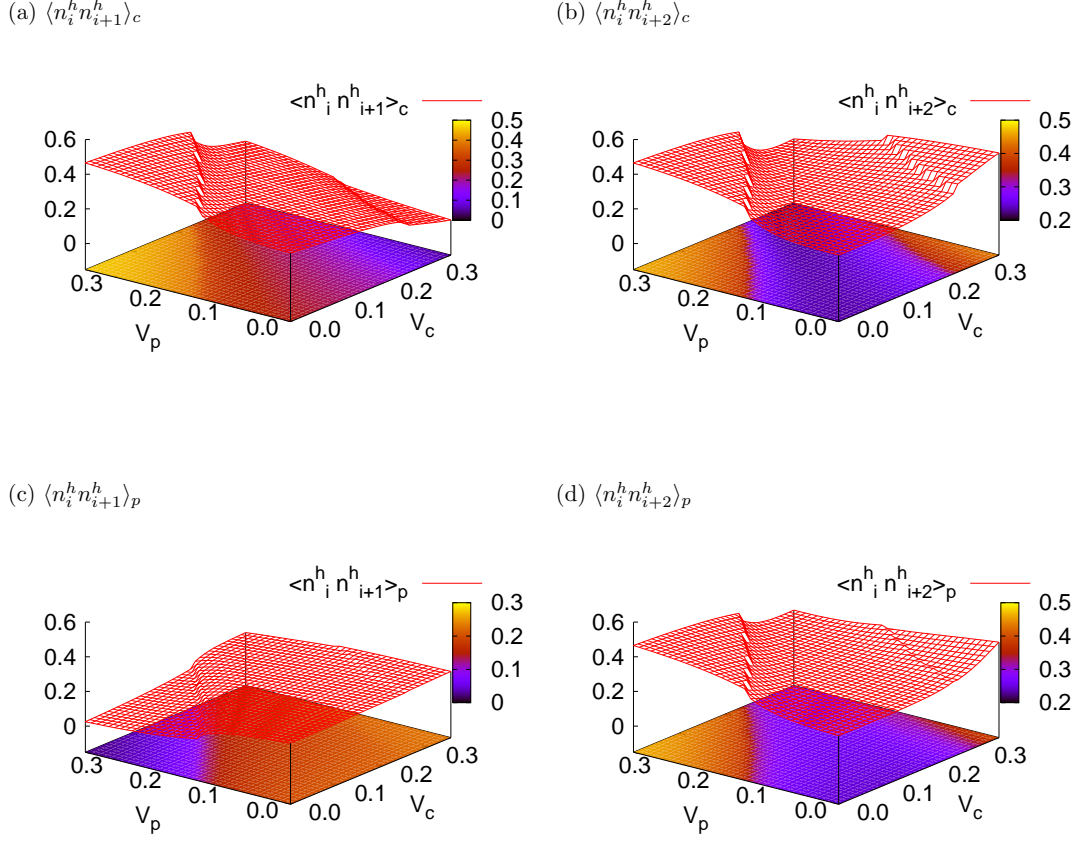

(d) $\langle n_i^h n_{i+2}^h \rangle_p$

FIG. 2: Hole-hole correlation functions as a function of V_c and V_p for $U = 0.7$ without electron-phonon couplings: (a) $\langle n_i^h n_{i+1}^h \rangle_c$ and (b) $\langle n_i^h n_{i+2}^h \rangle_c$ are correlation functions along vertical bonds. (c) $\langle n_i^h n_{i+1}^h \rangle_p$ and (d) $\langle n_i^h n_{i+2}^h \rangle_p$ are correlation functions along diagonal bonds.

that we cannot find the horizontal-stripe CO phase in any combination of V_c and V_p, which is observed experimentally in the θ-RbZn salt at low temperature.

Below we mainly use $V_c = 0.31$, $V_p = 0.27$ in phase I of Fig. 3, where this ratio of V_c/V_p is regarded as appropriate for the θ-RbZn salt.[23] To check whether these values themselves are appropriate, we have calculated the optical conductivity spectra by means of the continued fraction expansion to show them in Fig. 4.[24] It is found that for both polarizations E they have a broad peak around $\omega \sim 0.4$ eV and the conductivity for $E\|a$ is larger than that for $E\|c$, which are consistent with the experimental findings.[25] Therefore, these interaction strengths are quite reasonable.

B. Case with electron-phonon couplings

Each of the three kinds of electron-phonon couplings is studied at the particular point of $V_c = 0.31$ and $V_p = 0.27$ by the exact diagonalization. Because we need to obtain the displacements consistently with bond densities, we used the smaller system of the 12 sites hereafter and

compared some results with those of the 16-site cluster. The conclusion is found to be unchanged and, in fact, understood from the perturbation theory from the strong-coupling limit, as discussed later.

First, we see the effect of molecular rotations (s_{p4}). The s_{p4}-dependence of the modulations of transfer integrals and the hole densities is shown in Fig. 5(a) with $s_c = s_{p1} = 0$ fixed. For small s_{p4}, as all the phonons are undistorted and the hole densities are uniform ($\langle n_i^h \rangle = 0.5$), the ground state remains the coexistent state of the vertical-stripe CO and the diagonal-stripe CO. With increasing s_{p4}, the system discontinuously changes at a critical point $s_{p4}^{cr} \sim 0.04$, to the CO state of broken symmetry. This CO pattern is the HCO-t_{p4} ($\langle n_1^h \rangle$, $\langle n_4^h \rangle \gg \langle n_2^h \rangle$, $\langle n_3^h \rangle$), which agrees with the experimental findings.[12] Therefore, the coupling with molecular rotations (s_{p4}) plays an important role to realize this HCO state. It is noted that y_{p4} increases almost linearly after the critical point where the HCO-t_{p4} state is stable. This discontinuous change at the critical point would be caused by the finite-size effect: the undistorted state is stabilized by quantum tunneling between different CO states, but its energy gain would vanish in the
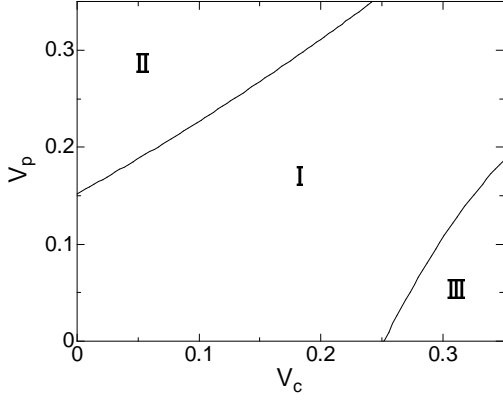
FIG. 3: Phase diagram for $U = 0.7$ without electron-phonon couplings. All phases are uniform, but the dominant hole-hole correlations are different. The vertical-stripe CO and the diagonal-stripe CO coexist in phase I. The vertical-stripe CO is the largest correlation in phase II, while the diagonal-stripe CO is the largest correlation in phase III.
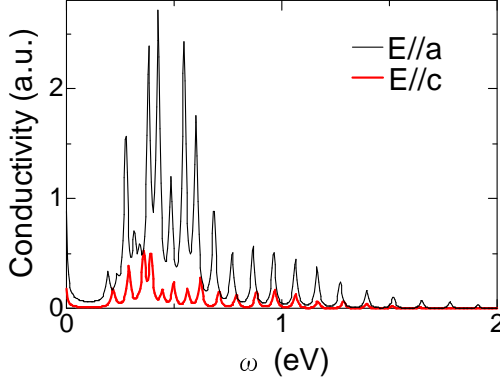

FIG. 4: (Color online) Optical conductivity spectra of the model (1) on the 4×4-site cluster for electric fields, $E\|a$ (thin line) and $E\|c$ (thick line). We use $U = 0.7$, $V_c = 0.31$ and $V_p = 0.27$. The δ-functions appearing in the continued fraction expansion are broadened with width $\eta=0.01$.

thermodynamic limit. In fact, y_{p4} rises up linearly by infinitesimal s_{p4} in mean-field calculations,[26] so we guess that the critical point approaches zero in the thermodynamic limit.

Next, we consider the effect of translations in the c-direction (s_c). For large s_c, they also stabilize the HCO-t_{p4} state as shown in Fig. 5(b). In the case of s_c, the charge disproportionation between the hole-rich sites ($\langle n_1^h \rangle$, $\langle n_4^h \rangle$) and the hole-poor sites ($\langle n_2^h \rangle$, $\langle n_3^h \rangle$) is smaller than the case of s_{p4}, but the translations in the c-direction further stabilize the HCO-t_{p4}.

The situation regarding s_{p1} is quite different from the cases of s_{p4} and s_c. The s_{p1}-dependence of the transfer modulations and the hole densities at four sites is shown in Fig. 5(c). In the presence of only y_{p1}, which represents

translations in the a-direction, the CO pattern is still a horizontal-type but the holes are localized on the t_{p1} and t_{p3} bonds. Thus, the experimental findings are not reproduced if only s_{p1} exists.

From Figs. 5(a)-5(c), we conclude that the effects of molecular translations in the c-direction (s_c) and molecular rotations (s_{p4}) are stronger than that of translations in the a-direction (s_{p1}) in this salt. We also come to the same conclusion in the other phases of Fig. 3. In Fig. 6, we perform the same calculations (except for the parameters shown) as in Fig. 5(a) for phases II and III. The s_{p4}-induced HCO-t_{p4} state is stable in both of phases II and III when s_{p4} is large enough. Therefore, this characteristic phonon-induced feature is widely obtained on the V_c-V_p plane, including $V_c = V_p = 0$ (irrespective of hole-hole correlations in the uniform ground state without electron-phonon couplings).

Finally, we simultaneously take the three kinds of displacements into account. Considering a situation with thermal- or pressure-induced expansion or compression, we vary intersite Coulomb interactions. In Fig. 7, we show the modulations of transfer integrals and the hole densities as a function of nearest-neighbor Coulomb interactions. For small r, only y_{p1} is finite with y_c and y_{p4} being zero. This situation is quite similar to Fig. 5(c), and hence the most stable state is the HCO-t_{p1}&t_{p3}. As r approaches unity, which is a realistic value for θ-RbZn, the experimentally observed HCO-t_{p4} state becomes more stable than the HCO-t_{p1}&t_{p3} by gradually increasing y_c and y_{p4} and rapidly decreasing y_{p1}. In the vicinity of $r = 1$ for $s_c = 0.05$, $s_{p1} = 0.17$, and $s_{p4} = 0.06$, y_c and y_{p4} approximately correspond to the low-symmetry structure of θ-RbZn at low temperature.

From the X-ray structure analysis,[12] the molecular translations in the c- and a-directions are found to be $u_c \sim 0.13$Å and $u_{p1} \sim 0.15$Å, and the corresponding distortions are $y_c = 0.0185$eV and $y_{p1} = 0.0735$eV. They give $\alpha_c \sim 0.14$eV/Å and $\alpha_{p1} \sim 0.47$eV/Å. The present coupling strengths $s_c = 0.05$eV and $s_{p1} = 0.17$eV lead to $K_c \sim 0.38$eV/Å^2 and $K_{p1} \sim 1.32$eV/Å^2. A rough estimation of phonon frequencies by $\omega_\mu = \sqrt{K_\mu/m}$ with m being the reduced mass of two BEDT-TTF molecules shows $\omega_c \sim 23$cm^{-1} and $\omega_{p1} \sim 43$cm^{-1}, which are quite reasonable values.[17]

As r further increases beyond two, all modulations approach zero. In particular, y_{p1} decreases monotonically. We explain these behaviors with a perturbation theory from the strong-coupling limit in the following section. Thus, electron-phonon interactions are crucial to stabilize the horizontal-stripe CO and to realize the low-symmetry structure of θ-RbZn at low temperature. All these results are consistent with mean-field studies of the same model.[26]
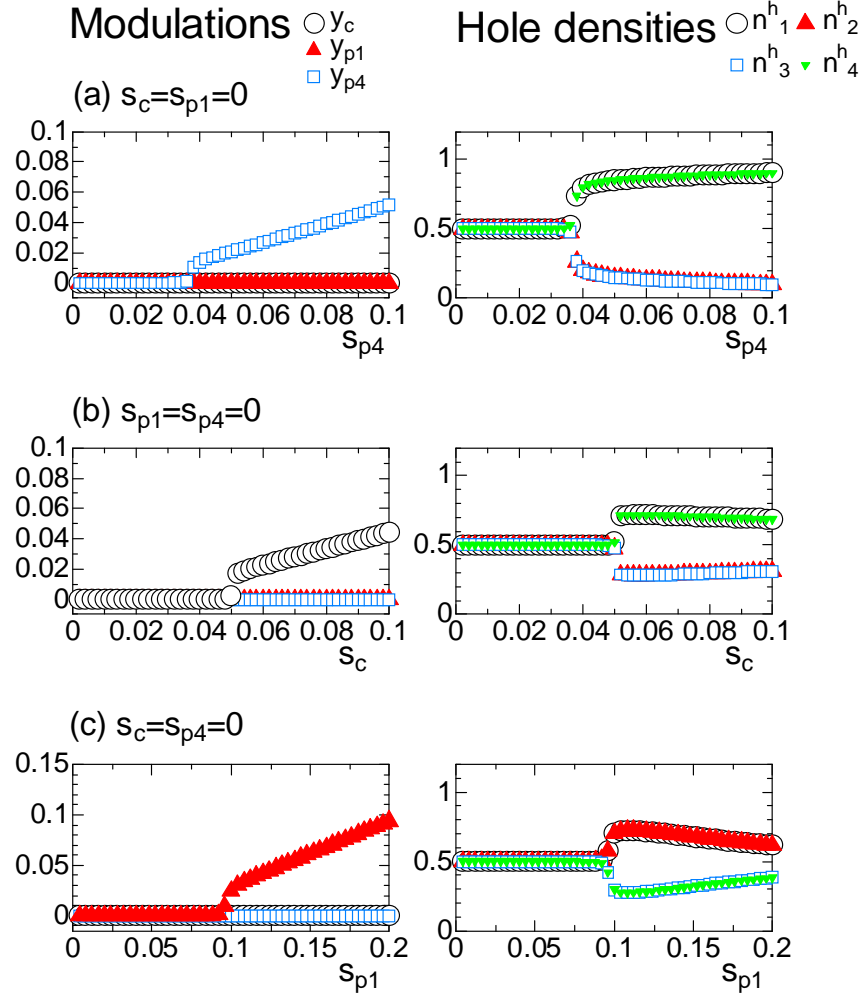
FIG. 5: (Color online) (a) s_{p4}-dependence of modulations of transfer integrals (left) and hole densities (right) for $s_c=s_{p1}=0$, (b) their s_c-dependence for $s_{p1}=s_{p4}=0$, and (c) their s_{p1}-dependence for $s_c=s_{p4}=0$, with $U=0.7$, $V_c=0.31$ and $V_p=0.27$.

IV. DISCUSSION

In this section, we consider why the HCO-t_{p4} is the most stabilized by the electron-phonon couplings. It is easily understood in the strong-coupling limit. We assume that, in this limit, the holes are perfectly localized on the t_{p4} bonds, namely $\langle n_1^h \rangle = \langle n_4^h \rangle = 1$ as shown in Fig. 1(b). In the ordinary perturbation theory, the second- and third-order contributions to the energy per site read

$$E_2 = -\frac{t_{c1}^2 + t_{c2}^2}{2V_c} - \frac{t_{p1}^2 + t_{p3}^2}{2(2V_c - V_p)}$$
$$+ \frac{2t_{p4}^2}{U - V_p}\left\{\langle \mathbf{S}_i \cdot \mathbf{S}_j \rangle - \frac{1}{4}\right\}, \tag{5}$$

$$E_3 = -\frac{(t_{p1} + t_{p3})t_{c2}t_{p2}}{V_c(2V_c - V_p)} + \frac{2(t_{p1} + t_{p3})t_{c1}t_{p4}}{V_c(2V_c - V_p)}\left\{\langle \mathbf{S}_i \cdot \mathbf{S}_j \rangle + \frac{1}{4}\right\}$$
$$+ \frac{2(t_{p1} + t_{p3})t_{c1}t_{p4}}{V_c(U - V_p)}\left\{\langle \mathbf{S}_i \cdot \mathbf{S}_j \rangle - \frac{1}{4}\right\}$$
$$+ \frac{2(t_{p1} + t_{p3})t_{c1}t_{p4}}{(2V_c - V_p)(U - V_p)}\left\{\langle \mathbf{S}_i \cdot \mathbf{S}_j \rangle - \frac{1}{4}\right\}, \tag{6}$$

where $\mathbf{S}_i$ is the $S = 1/2$ spin operator at the i-th site on the t_{p4} bond. In the strong-coupling limit, the one-dimensional half-filled chain is formed along the t_{p4} bonds and $\langle \mathbf{S}_i \cdot \mathbf{S}_{i+1} \rangle = -\ln 2 + 1/4 \simeq -0.443$ is the exact ground-state energy of the isotropic $S = 1/2$ Heisenberg
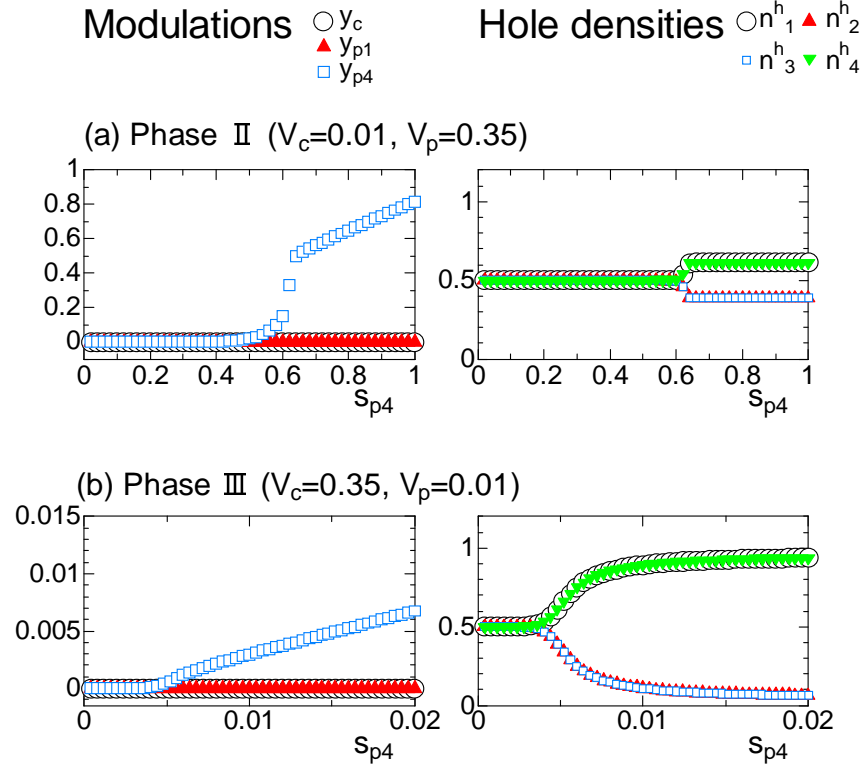
FIG. 6: (Color online) s_{p4}-dependence of modulations of transfer integrals (left) and hole densities (right), (a) in phase Ⅱ ($V_c = 0.01$, $V_p = 0.35$), and (b) in phase Ⅲ ($V_c = 0.35$, $V_p = 0.01$), for U=0.7 with $s_c=s_{p1}=0$ fixed.

chain. According to the third term in Eq. (5), there is energy gain from spin fluctuations, so that the ground-state energy of the HCO-t_{p4} state is further lowered by increasing $|t_{p4}|$. On the other hand, because all terms in Eq. (6) are positive, E_3 represents energy loss. When $|t_{p4}|$ becomes large, $|t_{c1}|$ becomes small to reduce the energy loss. From the relations (3), $|t_{c2}|$ becomes large and $|t_{p2}|$ becomes small.

Equations (5) and (6) can be rewritten as

$$E_2 \; \propto \; a + c_1 \; t_{p4}^{\mathrm{HT}} \; y_{p4} \; , \tag{7}$$

$$E_3 \; \propto \; b + c_2 \; t_c^{\mathrm{HT}} \; y_{p4} + c_3 \; t_{p4}^{\mathrm{HT}} \; y_c \; , \tag{8}$$

where a, b and c_i ($i = 1, 2, 3$) are independent of y_μ, and $t_{p4}^{\mathrm{HT}} < 0 < t_c^{\mathrm{HT}}$. Note that we ignore y_μ^2 in deriving the above equations, and the coefficients c_i are positive under the condition $2V_c \geq V_p$. We can infer from Eq. (7) that y_{p4} increases linearly as a function of s_{p4} when the ground state is the HCO-t_{p4} state. Because of the high symmetry with respect to $y_{p1} \leftrightarrow -y_{p1}$, Eqs. (7) and (8) are independent of y_{p1}. Once the distortions y_{p4} and y_c are substantially large, however, the distortion y_{p1} is numerically found to stabilize the HCO-t_{p4} further.

Before closing this section, we make a brief comment on the spinless fermion case.[27] In the $U \to \infty$ limit of the model(1), the HCO state becomes unstable even if the modulations of the transfer integrals are introduced

because the energy gain from spin fluctuations is absent. Thus we demonstrate that cooperative effects of electron correlations and electron-phonon couplings are important in the θ-RbZn salt. The stability of the HCO state relative to the diagonal CO state suggested in the spinless fermion case without electron-phonon couplings[27] might be caused by the absence of phase factors, which are present if the $U \to \infty$ limit is naively taken.

V. SUMMARY

We have investigated the cooperative effects of electron correlations and lattice distortions on the charge ordering in the θ-RbZn salt. By means of the exact-diagonalization method for systems with up to 16 sites, we have calculated the hole-hole correlation functions, the hole densities and the modulations of transfer integrals to clarify the role of electron-phonon couplings in this salt.

In the absence of electron-phonon interactions, there appear three uniform phases characterized by quantum tunneling between the vertical-stripe COs, that between the diagonal-stripe COs, and that between the vertical- and the diagonal-stripe COs. It is found that all of these phases are changed into the horizontal-stripe CO
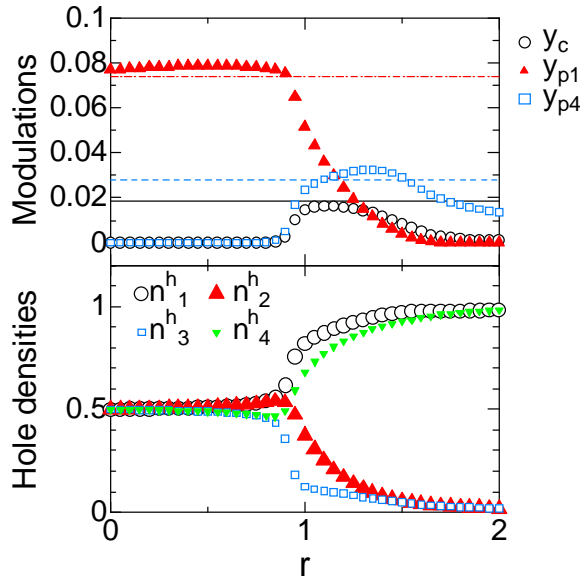
FIG. 7: (Color online) Three kinds of transfer modulations and hole densities at four sites for $U = 0.7$, $V_c = 0.31r$ and $V_p = 0.27r$. Coupling strengths are fixed at $s_c = 0.05$, $s_{p1} = 0.17$ and $s_{p4} = 0.06$. The solid (dashed-dotted) line in the upper panel represents the magnitude of the molecular translations in the $c(a)$-direction in the low-symmetry structure of θ-RbZn at low temperature.[12] The dashed line represents the magnitude of the molecular rotations in this structure.

by the introduction of electron-phonon couplings relevant to the θ-RbZn salt. We can mostly reproduce the low-symmetry structure of θ-RbZn at low temperature by using the model based on the high-symmetry structure at high temperature and by choosing the coupling strengths appropriately.

We conclude that the structural deformation assists the horizontal-stripe CO that is experimentally found.[12] In particular, the effects of molecular translations in the c-direction and molecular rotations are found to be stronger than that of translations in the a-direction. Thus, electron-phonon couplings are significant to stabilize the HCO-t_{p4} and to realize the low-symmetry structure of θ-RbZn. Otherwise the long-range Coulomb interactions favored a different CO pattern. With the help of the perturbation theory from the strong-coupling limit, we easily understand the mechanism for stabilizing the HCO-t_{p4} state and the linearly increasing y_{p4} and y_c modulations.

* Electronic address: satoshi@ims.ac.jp
[1] T. Ishiguro, K. Yamaji and G. Saito, *Organic Superconductors* (Springer, Heidelberg, 1998).
[2] J. M. Williams, J. R. Ferraro, R. J. Thorn, K. D. Carlson, U. Geiser, H. H. Wang, A. M. Kini and M.-H. Whangbo, *Organic Superconductors (Including Fullerenes: Synthesis, Structure, Properties, and Theory)* (Prince Hall, Englewood Criffs, NJ, 1992).
[3] Y. Shimizu, K. Miyagawa, K. Kanoda, M. Maesato and G. Saito, Phys. Rev. Lett. **91**, 107001 (2003).
[4] K. Kanoda, Physica C **282-287**, 299 (1997).
[5] M. Kino and H. Fukuyama, J. Phys. Soc. Jpn. **65**, 2158 (1996).
[6] H. Seo, J. Phys. Soc. Jpn. **69**, 805 (2000).
[7] S. Mazumdar, R. T. Clay and D. K. Campbell, Phys. Rev. B **62**, 13400 (2000).
[8] R. T. Clay, S. Mazumdar and D. K. Campbell, J. Phys. Soc. Jpn **71**, 1816 (2002).
[9] H. Seo, J. Merino, H. Yoshioka and M. Ogata, J. Phys. Soc. Jpn. **75**, 051009 (2006); and references therein.
[10] H. Mori, S. Tanaka and T. Mori, Phys. Rev. B **57**, 12023 (1998).
[11] H. Mori, S. Tanaka, T. Mori, A. Kobayashi and H. Kobayashi, Bull. Chem. Soc. Jpn **71**, 797 (1998).
[12] M. Watanabe, Y. Noda, Y. Nogami and H. Mori, J. Phys. Soc. Jpn. **73**, 116 (2004).
[13] K. Miyagawa, A. Kawamoto and K. Kanoda, Phys. Rev. B **62**, R7679 (2000).
[14] R. Chiba, H. Yamamoto, K. Hiraki, T. Takahashi and T. Nakamura, J. Phys. Chem. Solids **62**, 389 (2001).
[15] H. Tajima, S. Kyoda, H. Mori and S. Tanaka, Synth. Met. **120**, 757 (2001).
[16] K. Yamamoto, K. Yakushi, K. Miyagawa, K. Kanoda and A. Kawamoto, Phys. Rev. B **65**, 85110 (2002).
[17] S. Iwai, K. Yamamoto, A. Kashiwazaki, F. Hiramatsu, H. Nakaya, Y. Kawakami, K. Yakushi, H. Okamoto, H. Mori and Y. Nishio, Phys, Rev. Lett. **98**, 097402 (2007)
[18] L. Ducasse, F. Fritsch and F. Caster, Synth. Met. **85**, 1627 (1997).
[19] Y. Imamura, S. Ten-no, K. Yonemitsu and Y. Tanimura, J. Chem. Phys. **111**, 5986 (1999).
[20] T. Mori, Bull. Chem. Soc. Jpn. **73**, 2243 (2000).
[21] T. Mori, Bull. Chem. Soc. Jpn. **71**, 2509 (1998); T. Mori, H. Mori, and S. Tanaka, Bull. Chem. Soc. Jpn. **72**, 179 (1999); T. Mori, Bull. Chem. Soc. Jpn. **72**, 2011 (1999).
[22] J. Merino, H. Seo and M. Ogata, Phys. Rev. B **71**, 125111 (2005).
[23] T. Mori, J. Phys. Soc. Jpn. **72**, 1469 (2003).
[24] E. Dagotto, Rev. Mod. Phys. **66**, 763 (1994).
[25] H. Tajima, S. Kyoden, H. Mori and S. Tanaka, Phys. Rev. B **62**, 9378 (2000).
[26] Y. Tanaka and K. Yonemitsu, J. Phys. Soc. Jpn. **76**, No. 5 (2007).
[27] C. Hotta, N. Furukawa, A. Nakagawa and K. Kubo, J. Phys. Soc. Jpn. **75**, 123704 (2006).